Journal of Power Sources 196 (2011) 9696–9701

Contents lists available at ScienceDirect

Journal of Power Sources

journal homepage: www.elsevier.com/locate/jpowsour

Implications of the first cycle irreversible capacity on cell balancing for Li_2MnO_3–$LiMO_2$ (M = Ni, Mn, Co) Li-ion cathodes

W.C. West[a,*], R.J. Staniewicz[b], C. Ma[b], J. Robak[b], J. Soler[a], M.C. Smart[a], B.V. Ratnakumar[a]

[a] Jet Propulsion Laboratory, California Institute of Technology, Pasadena, CA 91109, United States
[b] Saft America Inc., Space and Defense Division – US, 107 Beaver Court, Cockeysville, MD 21030, United States

ARTICLE INFO

Article history:
Received 15 June 2011
Received in revised form 13 July 2011
Accepted 14 July 2011
Available online 23 July 2011

Keywords:
Irreversible capacity
MoS_2
Li-ion
Cathode
Cell balancing

ABSTRACT

Much of the research on lithium-ion cathodes consisting of layered solid solutions of Li_2MnO_3–$LiMO_2$ (M = Mn, Co, Ni) has focused on identifying the causes of the irreversible capacity loss on the first cycle. However, a key issue that must be addressed is whether the high irreversible capacity observed seen on the first cycle is associated with intercalated lithium at the anode, or if it is associated with irretrievable capacity (i.e., film formation, and/or decomposition reactions). To this end, we have quantified the amount of utilizable lithium that is made available for the anodes when employing Li_2MnO_3–$LiMO_2$ as cathodes. Using a MoS_2 anode lithiation plateau transition as a reference point to the amount of lithium transferred to the anode during charge, it has been shown that almost none of the cathode irreversible charge capacity resulted in lithiation of the anode. Further, by reacting charged graphitic anodes that were retrieved from C anode–$Li_{1.2}Ni_{0.175}Co_{0.1}Mn_{0.52}O_2$ cathode cells with water to generate H_2 gas to measure the active amount of lithium in the anode, we confirmed the results with the MoS_2 titration experiments, demonstrating that lithium released from the cathode during the first charge is not proportionate to the cathode charge capacity.

1. Introduction

The lithium-ion cathode materials system comprising layered solid solutions of Li_2MnO_3–$LiMO_2$ (M = Mn, Co, Ni) has attracted significant interest for several years due to its high specific capacity of upwards of 240–280 mAh g^{-1} between 4.8 V and 2 V [1–4]. Unlike the more conventional $LiCo_xNi_{(1-x)}O_2$ cathode materials, the Li_2MnO_3–$LiMO_2$ solid solution cathodes exhibit a large irreversible capacity on the first charge, of as much as 40–100 mAh g^{-1} depending on the composition of the mixed metal oxides and surface treatments of the material. It is generally accepted that the irreversible capacity is associated with the removal of oxygen from the cathode accompanied by diffusion of transition metal ions from surface to bulk where they occupy vacancies created by lithium removal [5]. This capacity loss can be partly reduced by the addition of cathode dopants [6] or by preparing the cathode particles with thin coatings [7–10] though the irreversible capacity loss is a persistent feature of this attractive cathode materials system.

While much of the research on layered solid solutions of Li_2MnO_3–$LiMO_2$ has focused on identifying the causes of the irreversible capacity loss and methods to help mitigate the effect at the cathode, a key question must be addressed before this materials system can be infused into a lithium-ion cell manufacturing line: Does the first cycle excess charge capacity result in some fraction of lithiation of the anode? In a practical cell either with a graphitic anode or with a Li alloy anode, the anode and cathode loadings must be carefully balanced both in terms of irreversible capacities and reversible lithium capacities to maximize cell specific energy and to avoid lithium metal plating on the anode when the cathode loading high is relative to the anode. Given that a significant fraction of irreversible specific charge capacity, upwards by 15–40%, is generated on the first charge for these cathodes, it is imperative to understand the implications of this capacity with regard to the anode design. Unfortunately, the majority of the studies that have been performed on these materials to date have involved the use of lithium metal anodes, and have not addressed the nature of the irreversible capacity loss and the implications that this has upon electrode balancing issues (i.e., cathode to anode ratio).

To this end, we have carried out a series of experiments to quantify the amount of lithium transported to the anodes during the first charge when employing $Li_{1.2}Ni_{0.175}Co_{0.1}Mn_{0.52}O_2$ as a cathode. We have chosen two separate approaches to elucidate the nature of the irreversible cathode capacity in terms of anode effects. First, we have built full cells using MoS_2 as the anode, taking advantage of the relatively high lithium reduction potential of MoS_2 to avoid the complications associated with solid electrolyte interphase (SEI)

* Corresponding author. Tel.: +1 818 354 0053; fax: +1 818 393 6951.
E-mail address: william.c.west@jpl.nasa.gov (W.C. West).

0378-7753/$ – see front matter © 2011 Elsevier B.V. All rights reserved.
doi:10.1016/j.jpowsour.2011.07.050

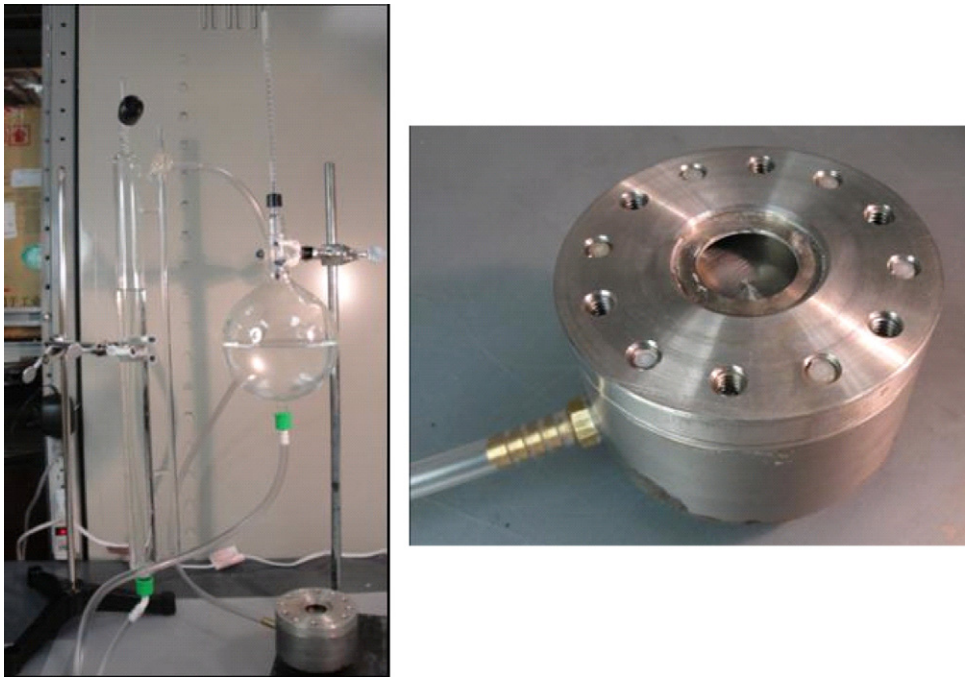

Fig. 1. Experimental apparatus used for reacting lithiated graphite anodes and capturing and measuring liberated H_2 gas.

film formation from the electro-reduction of the electrolyte species [11]. Additionally and importantly, MoS_2 has easily identifiable lithiation plateaus at about 1.2 V and 0.6 V vs. Li/Li^+ with an abrupt transition near $Li_{1.5}MoS_2$. This transition can be used to accurately track the degree of lithium inserted into the anode during cathode charging.

Second, we have prepared experimental cells consisting of $Li_{1.2}Ni_{0.175}Co_{0.1}Mn_{0.52}O_2$ cathodes and graphitic anodes, performed the formation cycling of the cells which was then followed by a final charge step prior to disassembling the cells and harvesting the charged anodes. These anodes were reacted with deionized water with the intent of generating H_2 gas which can be used to quantify the amount of lithium in the anode providing a separate and independent comparison to the MoS_2 titration experiments.

2. Experimental

2.1. Layered Li_2MnO_3–$LiMO_2$ (M = Ni, Mn, Co) cathode and MoS_2 electrochemical studies

X-ray diffraction (XRD) measurements were carried out using a Siemens D500 diffractometer run in the theta-2 theta geometry, with a Cu anode (λ = 1.541 Å) at an accelerating voltage of 40 kV and a tube current of 20 mA. Crystalline Si powder was added as a standard to the cathode powder for the XRD measurements. $Li_{1.2}Ni_{0.175}Co_{0.1}Mn_{0.52}O_2$ foils were prepared by spray coating Al foil substrates with slurries of 80 wt.% cathode powder ($Li_{1.2}Ni_{0.175}Co_{0.1}Mn_{0.52}O_2$, Toda), 10 wt.% C black (Shawinigan), and 10 wt.% poly(vinylene difluoride) (PVDF) binder (Sigma–Aldrich, MW_{avg} = 534,000) in N-methyl-2-pyrrolidinone (NMP) (Sigma–Aldrich). The $Li_{1.2}Ni_{0.175}Co_{0.1}Mn_{0.52}O_2$, electrode active mass loading was 6–8 mg cm^{-2}. MoS_2 foils were prepared by spray coating Cu foil substrates with slurries of 80 wt.% MoS_2 (Alfa Aesar), 10 wt.% C black (Shawinigan), and 10 wt.% poly(vinylene difluoride) (PVDF) binder (Sigma–Aldrich, MW_{avg} = 534,000) in N-methyl-2-pyrrolidinone (NMP) (Sigma–Aldrich). The MoS_2 electrode active mass loading was 2–7 mg cm^{-2}. The electrodes were heat sealed in 20 μm Tonen separators. Three electrode spiral wound cells were prepared by winding the spray-coated 3.8 cm × 15.9 cm cathodes, 3.8 cm × 17.8 cm anodes around a poly(tetrafluoroethylene) (PTFE) mandrel. A 3.8 cm × 0.635 cm Li foil reference electrode was inserted between the anodes and cathodes toward the beginning of the winding. The spiral wound electrodes were placed in a glass vial, to which 5.00 ml 1 M $LiPF_6$ in ethylene carbonate:dimethyl carbonate:diethyl carbonate (EC:DMC:DEC) (1:1:1 vol.%) electrolyte was added. The glass vial containing the electrodes and electrolyte was then sealed in an outer glass assembly equipped with a Viton O-ring and clamp. Coin cell studies were performed by assembling the above electrodes in stainless steel CR2032 coin cell hardware with Al clad stainless steel cases at the cathode terminal with 100 μl of the above electrolyte. Multiple cell replicants were used to validate the reproducibility of the cell data. Three electrode full cell measurements were carried out such that the voltage on the $Li_{1.2}Ni_{0.175}Co_{0.1}Mn_{0.52}O_2$ cathode and MoS_2 anode were measured relative to the Li reference electrode.

2.2. Layered Li_2MnO_3–$LiMO_2$ (M = Ni, Mn, Co) cathode and graphite H_2 gas titration studies

Cathode foils were prepared by coating Al foil with a single side active material loading of 15–22 mg cm^{-2}, and balanced carbon anode foils were prepared by coating Cu foil with single side active material loading of 10–15 mg cm^{-2}. The cathode and anode were separated by 16 μm Tonen separator. The electrode assembly was placed in Al laminated pouch cell sheets, filled with 1 M $LiPF_6$ in EC:DMC:DEC (1:1:1 vol.%) electrolyte, and heat sealed. The cells were weighed, DC resistance and open circuit voltage of cell was measured and then the cell was soaked for 24 h at 35 °C.

After conditioning at 35 °C, the $Li_{1.2}Ni_{0.175}Co_{0.1}Mn_{0.52}O_2$–graphite cells were charged in successive cycles to 4.5 V, 4.6 V, and 4.7 V at C/10 rate at 35 °C and discharged through to 3 V. The pouch cells were then cut open on the corner for gas release by vacuum then re-sealed at the opening by heat sealer. The weight of the pouch cells was remeasured to verify there was still an excess of electrolyte inside pouch cells.

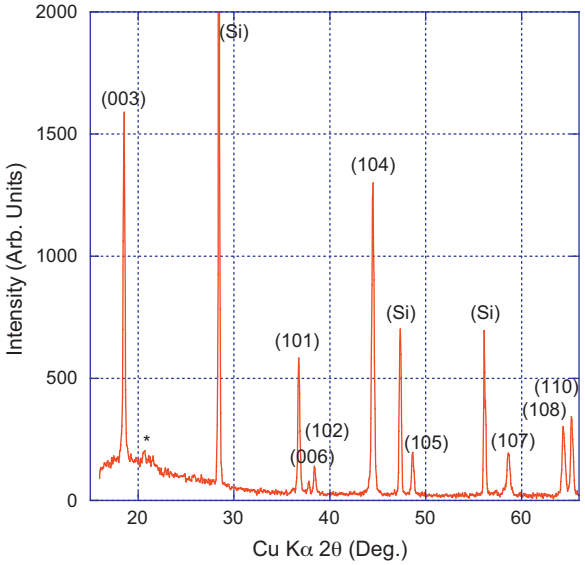

Fig. 2. X-ray powder diffraction pattern for $Li_{1.2}Ni_{0.175}Co_{0.1}Mn_{0.52}O_2$ cathode. Peaks associated with Si standard are labeled (Si) and the asterisk indicates superlattice ordering peak.

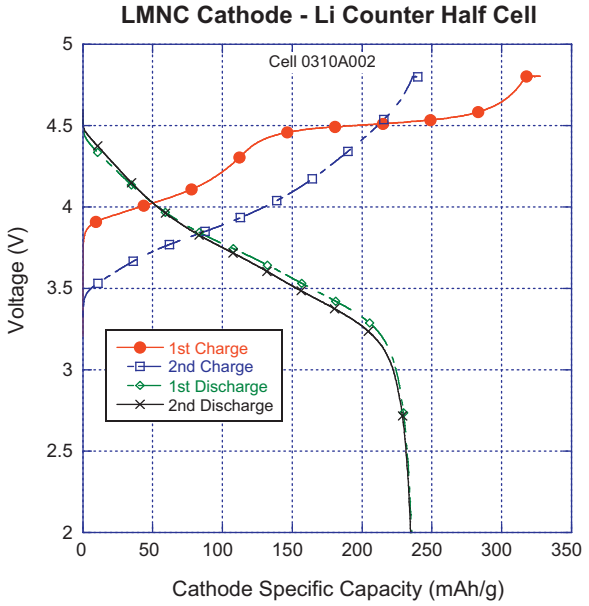

Fig. 3. Charge/discharge profiles of $Li_{1.2}Ni_{0.175}Co_{0.1}Mn_{0.52}O_2$ cathodes in half cell, coin cell configuration through two charge–discharge cycles.

At the fourth cycle, the cells were charged and discharged at room temperature. The cells were then charged for a fifth time at C/10 to 4.7 V at room temperature, and then disassembled in a dryroom. The charged graphite anodes were then placed in a steel vessel and reacted with deionized water in excess. The H_2 gas liberated from this reaction was collected, measured and the total volume of H_2 gas was corrected to standard temperature and pressure (STP) to calculate the electrochemical equivalent of Li in the lithiated graphite anode. The apparatus used to carry out these measurements are shown in Fig. 1.

3. Results and discussion

3.1. Layered Li_2MnO_3–$LiMO_2$ (M = Ni, Mn, Co) cathode and MoS_2 performance in half cells

The cathode powders were well-indexed to the expected layered-layered solid solution Li_2MnO_3–$LiMO_2$ (M = Ni, Mn, Co), with no additional unindexed diffraction peaks (Fig. 2). Weak peaks at 2θ of 21° to 25° that were not indexed to the R3m symmetry were consistent with cation ordering that occurs in the transition metal layer [12]. The typical performance of half cells prepared using $Li_{1.2}Ni_{0.175}Co_{0.1}Mn_{0.52}O_2$ cathodes and Li anodes in coin cell format, cycled at room temperature C/20 rates is shown in Fig. 3 for the first two cycles. The first charge was characterized by a smoothly sloping charge region up to 4.5 V followed by a well defined charge plateau occurring around 4.5–4.6 V. This voltage plateau on the first charge corresponds to the removal of oxygen from the cathode accompanied by diffusion of transition metal ions from surface to bulk where they occupy vacancies created by lithium removal [5].

The average first cycle specific charge capacity for 4 cells was 324 mAh g^{-1}, with an average first cycle specific discharge capacity of 236 mAh g^{-1}. Thus, the average first cycle irreversible capacity was 88 mAh g^{-1}. For the second and subsequent charges, the 4.5–4.6 V plateau disappeared and was replaced by a smoothly sloping charge with average specific charge capacity of 244 mAh g^{-1}, yielding a coulombic efficiency of about 97% on the second and subsequent cycles.

In order to understand the lithiation capacity of the MoS_2 anode, two sets of three electrode spiral wound cells were prepared with a MoS_2 working electrode, Li counter, and Li reference. The first discharge (or lithium intercalation into MoS_2) for both cells is shown in Fig. 4 (expressed as lithium content x in Li_xMoS_2). The lithiation of MoS_2 at a current density of 0.74 mA cm^{-2} resulted in two plateaus of 1.2 V and 0.6 V. The transition between the 2 plateaus, taken as 0.9 V vs. Li/Li^+ occurred at an average composition of $x = 1.50 \pm 0.04$ for Li_xMoS_2 corresponding to about 250 mAh g^{-1}. Julien [13] reports the transition between the 2 plateaus occurs at about $x = 1.2$, though others have shown that the transition and discharge profile is rate dependent [14].

3.2. Full cell studies

With the lithiation profile of MoS_2 characterized, particularly the composition at which the transition between the 2 distinct lithiation plateaus occurs, it was then possible to study the amount of

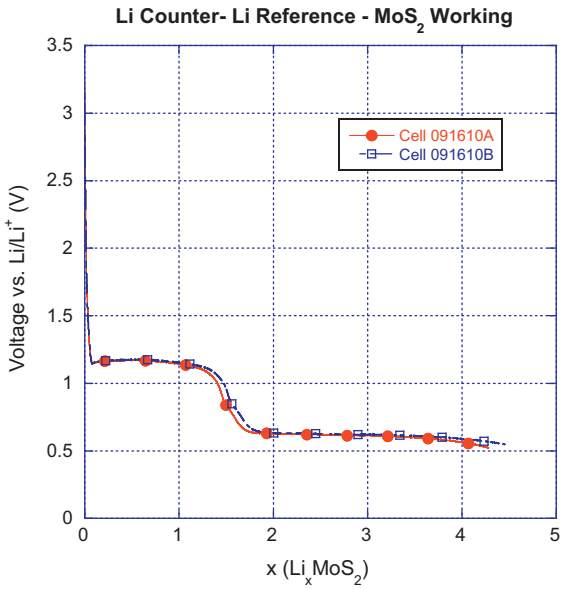

Fig. 4. Lithiation profiles of MoS_2 working electrodes in spiral wound half cell configuration.

Table 1
Apparent lithium content (x) in Li_xMoS_2 at 0.9 V transition as a function of cathode/anode mass ratio.

Cell ID	Cathode/anode mass ratio	x in Li_xMoS_2 at the 0.90 V transition	Cathode specific charge capacity prior to 0.9 V transition (mAh g^{-1})
110210A (Fig. 5)	2.55	2.01	132
110210B (Fig. 6)	2.12	2.03	160
102510F (Fig. 7)	1.20	2.08	289
091610D (Fig. 8)	1.04	2.07	331[a]

[a] Transition started but not completely reached before cathode was fully charged.

capacity removed from the layered Li_2MnO_3–$LiMO_2$ cathode and correlate it to the amount of lithium inserted into the MoS_2 anode. Four full cells with varying cathode to anode masses were prepared, as listed in Table 1. The intent of varying cathode–anode mass ratios was to assure the characteristic lithiation plateau transition at 0.9 V vs. Li/Li^+ would occur at various stages of de-lithiation of the cathode.

If all of the charge capacity corresponded to the release of lithium from the cathode and its subsequent insertion into the MoS_2 anode as lithium, then the Li_xMoS_2 0.9 V transition should always occur at $x = 1.5$ provided that the cathode–anode ratio was not designed overly anode-heavy which would result in all the cathode capacity being inserted before the 0.9 V transition could occur. If, as expected, the charge capacity of the cathode included (1) capacity associated with the formation of the anode SEI, (2) capacity associated with irreversible oxygen loss from the cathode, and (3) reversible lithium from the cathode, then the 0.9 V transition will apparently occur at $x > 1.5$ for Li_xMoS_2. However, the apparent x-value composition at which the transition occurs will necessarily depend on the cathode–anode ratios. This may be understood by considering that the relative amounts of capacity from the 3 contributions to cathode charge capacity will likely vary as a state of charge. To illustrate this point, two extreme cases in which the cathode–anode mass ratios are either high or ideally balanced are considered. In the case where the cathode–anode mass ratio is high, the charge capacity from the cathode may fully lithiate the MoS_2 anode to the 0.9 V transition before any capacity associated with the cathode oxygen loss occurs. In this situation, the x-value for Li_xMoS_2 will be only slightly greater than $x = 1.5$. In the case where the cathode–anode mass ratios is ideally balanced, all of the charge capacity from the cathode is captured by the anode at the very end of cathode charging at the precise value that anode voltage crosses the 0.9 V transition and as such the apparent x value in Li_xMoS_2 anode can then be used to fully estimate the relative contributions of cathode capacity from both irreversible (SEI and oxygen loss) and reversible de-lithiation processes.

Figs. 5–8 show the full cell charge profile for four cells with varying cathode-anode mass ratios (2.55, 2.12, 1.20, and 1.04 respectively) with the MoS_2 anode and $Li_{1.2}Ni_{0.175}Co_{0.1}Mn_{0.52}O_2$ cathode voltages displayed relative to the Li reference during the charge. In all four plots, the cathode specific capacity–voltage profile was in excellent agreement with coin cell studies, with the first charge 4.5–4.6 V plateau well resolved and the cathode charge capacity attaining an average value of 330 mAh g^{-1}.

In Figs. 5–7, the 0.9 V transition in the anode profile was clearly observed, while in Fig. 8 the voltage transition commenced but did not reach 0.9 V before the cell reached the fully charged state. The MoS_2 anode voltage for all four plots regardless of cathode–anode mass ratio all exhibited a slight uptick in voltage as the cell transitioned from constant current charging to the current taper/constant voltage step. It is likely that this slight positive change in anode voltage inflection is an artifact of the measurement system as the cycler transitioned from the constant current to constant voltage (current taper) mode.

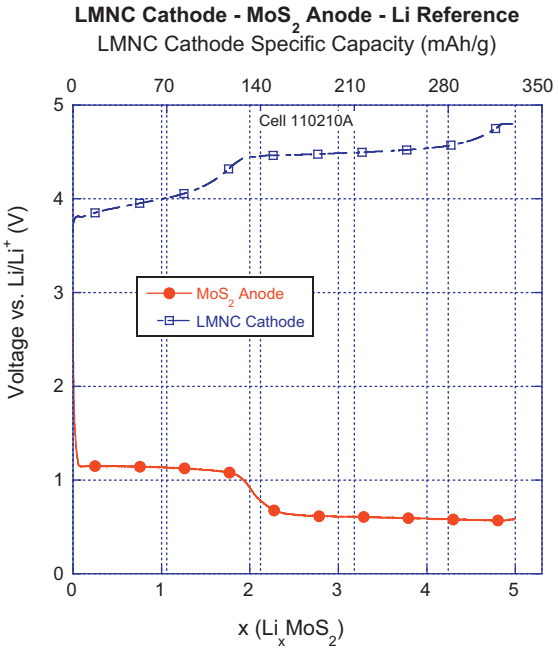

Fig. 5. Lithiation profiles of full cell $Li_{1.2}Ni_{0.175}Co_{0.1}Mn_{0.52}O_2$ cathode, MoS_2 anode, and Li reference in spiral wound cell configuration. Cathode–anode mass loading = 2.55.

In all 4 cells, the 0.9 V anode transition occurred at x-values significantly greater than 1.5, demonstrating that less than 100% of the charge capacity of the cathode was captured in the MoS_2 anode. In other words, the amount of lithium available at and intercalated into MoS_2 anode does not equate to the charge capacity at the cathode. Alternately, during the charging of the cathode, it is not entirely lithium that is being released. There is some other parallel process, likely the electrochemical generation of oxygen occurring at the cathode, which does not involve release of lithium ions. From the

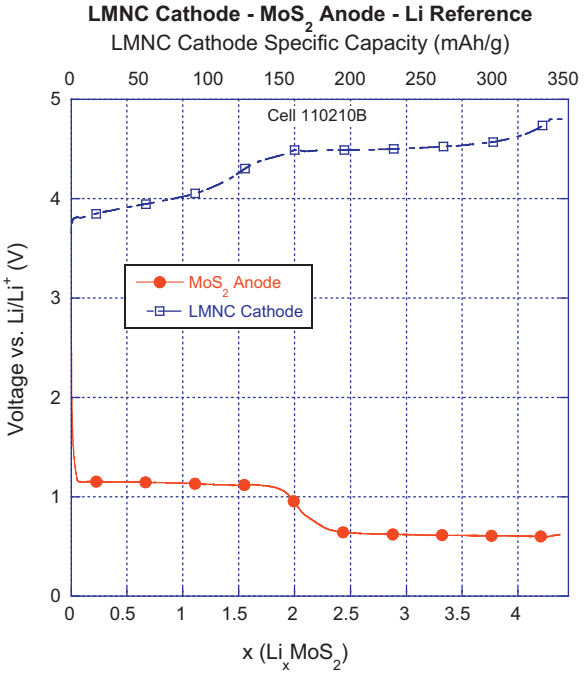

Fig. 6. Lithiation profiles of full cell $Li_{1.2}Ni_{0.175}Co_{0.1}Mn_{0.52}O_2$ cathode, MoS_2 anode, and Li reference in spiral wound cell configuration. Cathode–anode mass loading = 2.12.

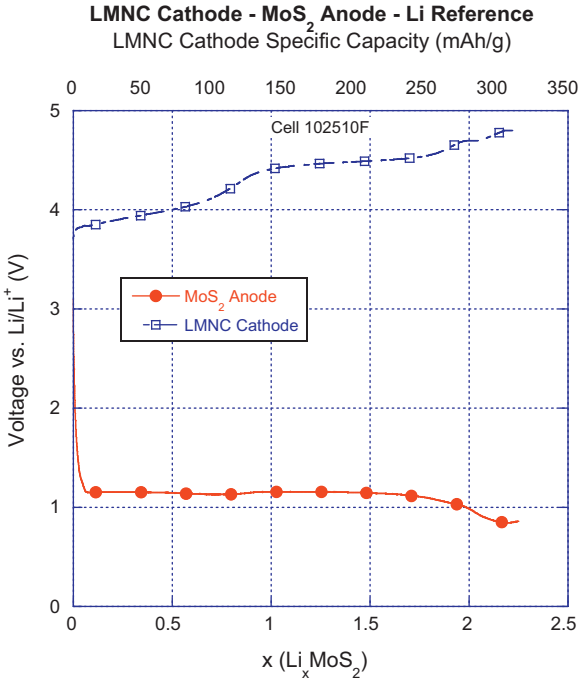

Fig. 7. Lithiation profiles of full cell $Li_{1.2}Ni_{0.175}Co_{0.1}Mn_{0.52}O_2$ cathode, MoS_2 anode, and Li reference in spiral wound cell configuration. Cathode–anode mass loading = 1.20.

cell data represented in Fig. 8 where the 0.9 V transition began very near to the end of the cell charging, it is possible to calculate the difference in cathode capacity and the amount of lithium delivered to the anode. For this cell, the capacity at the end of charge was 134 mAh, with a cathode active mass of 0.4046 g corresponding to a cathode specific charge capacity of 331 mAh g^{-1}. The anode transition to 0.9 V was extrapolated to a cell capacity of 134 mAh for an anode active mass of 0.3880 g, again as with other cells neglecting

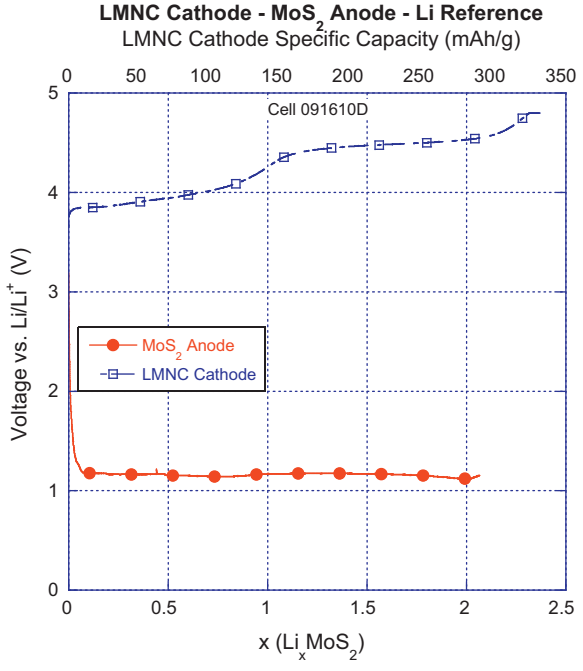

Fig. 8. Lithiation profiles of full cell $Li_{1.2}Ni_{0.175}Co_{0.1}Mn_{0.52}O_2$ cathode, MoS_2 anode, and Li reference in spiral wound cell configuration. Cathode–anode mass loading = 1.04.

the uptick in voltage at the current taper step. The difference in anode capacity between the expected transition at $Li_{1.5}MoS_2$ and the measured value of $Li_{2.07}MoS_2$ is 37 mAh. On a cathode basis, this results in the key finding that 91 mAh g^{-1} of the cathode specific charge capacity does not involve lithium species and thus does not lithiate the anode. The cell level data for the four cells is summarized in Table 1.

3.3. Full cell studies: Li titration via water reaction with lithiated anodes

As an alternative method to infer the amount of capacity removed from the layered Li_2MnO_3–$LiMO_2$ cathode and correlate it to the amount of lithium transferred into an anode, C–Li_2MnO_3–$LiMO_2$ cells were constructed, cycled, and then fully charged prior to disassembly and electrode harvesting as described in Section 2. By reacting the charged anode with deionized water in excess, the amount of H_2 gas generated can be used to estimate the amount of electrochemically active lithium in the anode, assuming the lithiated graphite reacts to completion following:

$$Li_xC + xH_2O \rightarrow xLiOH + (1/2)xH_2 + C$$

Two cells were prepared and tested, with the resultant data summarized in Table 2. It should be noted again that while the Li_2MnO_3–$LiMO_2$ cathode–MoS_2 anode cells were cycled at room temperature, the Li_2MnO_3–$LiMO_2$ cathode–graphite anode cells were first conditioned by cycling at +35 °C and then charged and discharged at room temperature for the final cycles. It is possible that other side reactions such as proton exchange or electrolyte decomposition can contribute to charge capacity particularly at elevated temperatures as shown by other groups [15].

Compared with the previous experimental cells in Figs. 3 and 5–8, the cathode first charge specific capacity was similar with an average of 334 mAh g^{-1}. After charging the cathode, the cells were disassembled, the anode was reacted with deionized water, and the amount of H_2 gas generated from the charged graphitic anode was measured. From these charged anode–water reaction measurements, assuming the formation of an anode SEI film consuming a specific capacity of 38 mAh g^{-1}, the amount of lithium in the charged anode was measured to correspond to an average of 240 mAh g^{-1}. Thus the average irreversible capacity from the Li titration experiments was 94 mAh g^{-1}. This irreversible, non-electrochemically active specific charge capacity value is very close to the value calculated from the MoS_2 anode studies (91 mAh g^{-1}).

It is thus clear from 2 independent studies that the lithium release from the layered solid solutions of Li_2MnO_3–$LiMO_2$ (M = Mn, Co, Ni) mixed metal oxide cathodes during the first charge is lower than may be estimated from their charge capacities. This would imply that a parallel process, possibly oxygen evolution through an electrochemical route, is occurring on these cathode surfaces. There will be accompanying redistribution of vacancies within the cathode for charge neutrality. A more intriguing question is on the issue of the likely reactions occurring at the anode, since the reactions involving Li species will account for only about 60–70% of the charge capacity. The question then would be: What is the anodic process conjugate to the oxygen release from the cathode? One possibility would be the recombination of oxygen at the anode; however, it is difficult to speculate on the reaction products and their effects. Clearly, further studies are warranted to understand the complexities in these cathodes.

Table 2
Summary of experimental data from Li titration studies.

Description	Cell ID: 77-1	Cell ID: 77-3	Average	Units
Total of 6 charges (ΣC)	1387	1467	1427	mAh g^{-1}
Total of 5 discharges (ΣD)	1014	1091	1053	mAh g^{-1}
Carbon SEI	42	40	41	mAh g^{-1}
Summation of capacity (sum) = $\Sigma C - \Sigma D -$ SEI	331	336	334	mAh g^{-1}
Volume of H_2 gas (corrected for STP)	17.8	19.3	18.6	ml
Li in anode as calculated from vol. of H_2 gas (Li)	234	246	240	mAh g^{-1}
Irreversible capacity not producing SEI or H_2	97	90	94	mAh g^{-1}

4. Conclusions

The nature of the first charge irreversible capacity in $Li_{1.2}Ni_{0.175}Co_{0.1}Mn_{0.52}O_2$ cathodes has been studied with regard to the amount of lithium transferred to the anode during the first charge. The reversible cathode discharge capacity of about 236 mAh g^{-1} is provided at the expense of a first cycle specific charge capacity of about 324 mAh g^{-1} resulting in an average irreversible cathode specific capacity of 88 mAh g^{-1}. Using a MoS_2 anode plateau transition as a reference point to estimate the amount of capacity transferred to the anode during charge, it has been shown that virtually none of the cathode irreversible charge capacity resulted in lithiation of the anode. By reacting charged graphitic anodes with water to generate H_2 gas to measure the active amount of lithium in the anode, the results of the MoS_2 titration experiments were confirmed, demonstrating the lack of lithiation capacity of the first cycle charge capacity beyond that which is recovered in subsequent discharges.

Acknowledgements

This work was carried out in part at the Jet Propulsion Laboratory, California Institute of Technology, under contract with the National Aeronautics and Space Administration. The authors wish to thank James Kulleck for carrying out the X-ray diffraction measurements. The authors acknowledge the funding support of NASA's Exploration Technology Development Program.

References

[1] Z. Lu, D.D. MacNeil, J.R. Dahn, Electrochem. Solid-State Lett. 4 (2001) A191.
[2] Z. Lu, D.D. MacNeil, J.R. Dahn, Electrochem. Solid-State Lett. 4 (2001) A200.
[3] S.-H. Kang, K. Amine, J. Power Sources 146 (2005) 654.
[4] C.S. Johnson, N. Li, C. Lefief, M.M. Thackeray, Electrochem. Commun. 9 (2007) 787.
[5] A.R. Armstrong, M. Holzapfel, P. Novak, C.S. Johnson, S.-H. Kang, M.M. Thackeray, P.G. Bruce, J. Am. Chem. Soc. 128 (2006) 8694.
[6] Y. Wu, A. Manthiram, Electrochem. Solid State Lett. 10 (2007) A151.
[7] Y. Wu, A. Manthiram, Solid State Ionics 180 (2009) 50.
[8] Y. Wu, A.V. Murugan, A. Manthiram, J. Electrochem. Soc. 155 (2008) A635.
[9] S.-H. Kang, M.M. Thackeray, Electrochem. Commun. 11 (2009) 748.
[10] S.H. Lee, B.K. Koo, J.-C. Kim, K.M. Kim, J. Power Sources 184 (2008) 276.
[11] E. Benevente, M.A. Santa Ana, F. Mendizabal, G. Gonzalez, Coord. Chem. Rev. 224 (1–2) (2002) 87.
[12] M.M. Thackeray, S.-H. Kang, C.S. Johnson, J.T. Vaughey, R. Benedek, S.A. Hackney, J. Mater. Chem. 17 (2007) 3052.
[13] C.M. Julien, Mater. Sci. Eng. R 40 (2003) 47.
[14] C. Feng, J. Ma, H. Li, R. Zeng, Z. Guo, H. Liu, Mater. Res. Bull. 44 (2009) 1811.
[15] A.R. Armstrong, A.D. Roberston, P.G. Bruce, J. Power Sources 146 (2005) 275.